Electronic Supplementary Material (ESI) for Chemical Communications.

Electronic Supplementary Information for

A cobalt–manganese layered oxide/graphene composite as an outstanding oxygen evolution reaction electrocatalyst

Hiroaki Kobayashi,‡*[a] Yuuki Sugawara,‡*[b] Takeo Yamaguchi,[b] and Itaru Honma[a]

[a] Institute of Multidisciplinary Research for Advanced Materials, Tohoku University,

2-1-1 Katahira, Aoba-ku, Sendai, Miyagi, 980-8577, Japan.

[b] Laboratory for Chemistry and Life Science, Institute of Innovative Research, Tokyo Institute of Technology, R1-17, 4259 Nagatsuta-cho, Midori-ku, Yokohama, Kanagawa 226-8503, Japan.

* Corresponding authors; E-mail: h.kobayashi@tohoku.ac.jp, sugawara.y.aa@m.titech.ac.jp

‡ H. K. and Y. S. contributed equally to this work.

Experimental

2.1. Chemicals

Potassium permanganate ($KMnO_4$), $CoCl_2$ and 2-propanol were purchased from Kanto Chemical Co., Inc. (Tokyo, Japan). Potassium hydroxide (KOH, 85%) was purchased from Wako Pure Chemical Industries, Ltd. (Osaka, Japan), and tetra-*n*-butylammonium bromide (*n*-Bu_4NBr) was purchased from Tokyo Chemical Industry Co., Ltd. (TCI) (Tokyo, Japan). Graphene nanopowder (G-10) was purchased from EM Japan Co., Ltd. (Tokyo, Japan); 5 wt% Nafion® solution (product number:

274704) was purchased from Sigma-Aldrich Japan K.K. (Tokyo, Japan), and its cation was exchanged by the addition of 0.1 M KOH aqueous solution. Iridium oxide (IrO_2, 75% Ir, product number: ELC-0110) was purchased from Tanaka Kikinzoku Kogyo (Tokyo, Japan). All other chemicals were purchased from Wako Pure Chemical Industries and used as received.

2.2. Catalyst Synthesis

CMO was synthesized *via* a modified protocol described in the literature.[1] First, n-Bu_4NMnO_4 powder (2 mmol) was slowly added to a $CoCl_2$ (2 mmol) solution in a mixture of 2-propanol (50 mL) and water (21.6 mL), followed by reflux for 3 h. The precipitates were collected by membrane filtration and washed with water and ethanol. CMO/G was similarly obtained by dispersing graphene nanopowder in the $CoCl_2$ solution before adding n-Bu_4NMnO_4. Caution: n-Bu_4NMnO_4 can react violently with itself (the MnO_4^- anion can oxidize the n-Bu_4N^+ cation) and possibly catch fire; hence, it should be handled with appropriate care and stored under appropriate conditions (*e.g.*, refrigerated conditions).

2.3. Material Characterizations

X-ray diffraction (XRD) patterns were collected using a D2 PHASER XE-T Edition (Bruker Japan K.K., Yokohama, Japan). Elemental analyses were performed using inductively coupled plasma atomic emission spectroscopy (ICP-AES) on an Optima 3300XL (PerkinElmer, Inc., MA, USA) and a CHN analyzer (Micro Corder JM10, J-Science Lab Co., Ltd., Kyoto, Japan). Transmission electron microscopy (TEM) images, energy dispersive X-ray spectrometry (EDS) elemental maps, and selected area electron diffraction (SAED) patterns were obtained using an ultrahigh-resolution TEM (EM-002B, Topcon Corporation, Tokyo, Japan). Brunauer–Emmett–Teller (BET) surface area analysis with N_2 and H_2O adsorbents were carried out using BELSORP-MINI X and BELSORP-MAX II (MicrotracBEL Corp., Osaka, Japan), respectively. X-ray photoelectron spectroscopy (XPS) analysis was performed using a PHI 5000 VersaProbe II system (Physical Electronics, Inc., MN, USA) with a mono-chromatic Al Kα source. Water contact angle measurements were carried out by the sessile drop method using a DSA100 (KRÜSS GmbH Wissenschaftliche Laborgeräte, Hamburg, Germany) at room temperature. Data of contact angles were obtained from the average of ten separated measurements for each sample.

2.4. Electrochemical Measurements

The OER activities of catalysts were evaluated on a potentiostat HZ-7000 (HOKUTO DENKO Corp., Tokyo, Japan) using a rotating disk electrode (RDE, disk area of 0.196 cm^2) with a glassy carbon disk as the working electrode (HR-301, HOKUTO DENKO Corp.). Fig. S4 shows the cell for the electrochemical measurements. Hg/HgO (1 M KOH) and Pt were used as reference and counter electrodes, respectively. The potential on the Hg/HgO electrode was converted to the reversible hydrogen electrode (RHE). The calibration of Hg/HgO was carried out as reported by Li *et al.*[2] and using the following equation:

$$E_{\mathrm{RHE}} = E_{\mathrm{Hg/HgO}} + 0.8929\ \mathrm{V} \tag{1}$$

The catalyst slurry of CMO/G was fabricated by mixing 2.0 mg CMO/G, 0.12 mL 3.3 wt% K^+ ion-exchanged Nafion®, 0.42 mL IPA and 1.46 mL water, followed by sonicating for 3 h. Eight microliters of the resulting slurry was coated on the RDE and dried by rotation at 600 rpm in air. The loading amount of CMO/G was maintained at 0.041 mg $\mathrm{cm}^{-2}{}_{\mathrm{disk}}$. The physically mixed CMO and graphene (CMO + G_PM) slurry was fabricated by mixing 5.0 mg CMO, 5.0 mg graphene and the same volumes of the abovementioned solvents and Nafion® solution for 3 min in an ice bath, followed by sonicating for 3 h. The CMO+G_PM electrode was fabricated as described above. The electrodes of bare CMO without graphene and pristine graphene without CMO were also prepared. The IrO_2 electrode was fabricated as described in our previous paper.[1]

The sample catalyst electrodes were pretreated by 10 cyclic voltammetry (CV) scans between 0.1 and 1.2 V vs. RHE at a scan rate of 50 mV s^{-1} without disk rotation. The oxygen evolution reaction (OER) activities of the catalysts were tested by CV scan sweeps between 1.2 and 1.8 V vs. RHE with a rotation speed of 1600 rpm at a scan rate of 10 mV s^{-1} in O_2-saturated 1 M KOH at ambient temperature. Reaction currents were calculated by taking the average of the forward and backward sweeps of the 10th cycle to cancel the capacitive currents. Electrolyte solutions were saturated by O_2 bubbling for 1 h before measurements. Ohmic losses were corrected by the following equation using the measured current (i) and electrolyte resistance (R), which was determined by ac impedance:

$$iR\text{-corrected } E = E_{\mathrm{RHE}} - iR \tag{2}$$

Electrochemical impedance spectroscopy (EIS) to measure the charge-transfer resistance (R_{ct}) was performed in a frequency range from 0.1 MHz to 0.1 Hz at 1.60 V with an amplitude of 5 mV.

The durability of the electrocatalytic performance was tested by potential cycling between 1.2 and 1.7 V at a scan rate of 100 mV s^{-1} in N_2-saturated 1 M KOH solution at ambient temperature.

Supplementary data

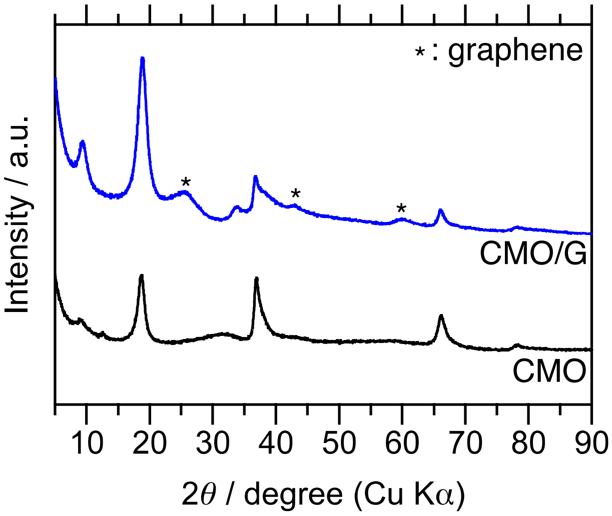

Fig. S1 XRD patterns of CMO/G and CMO.

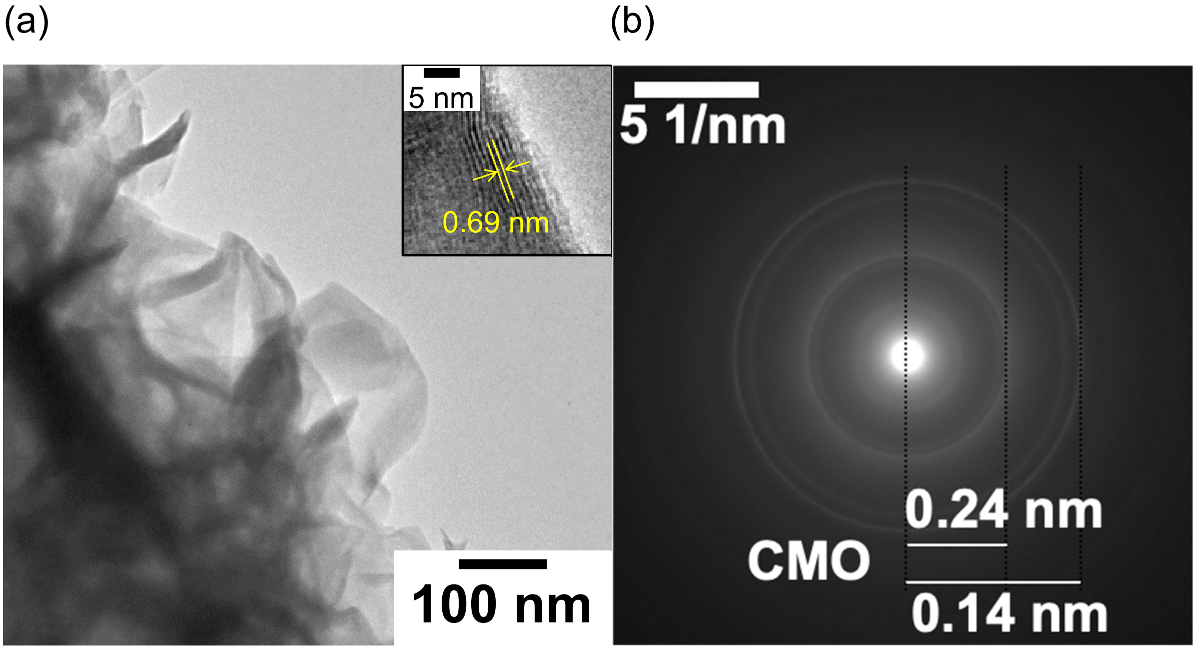

Fig. S2 (a) TEM and (b) SAED images of CMO.

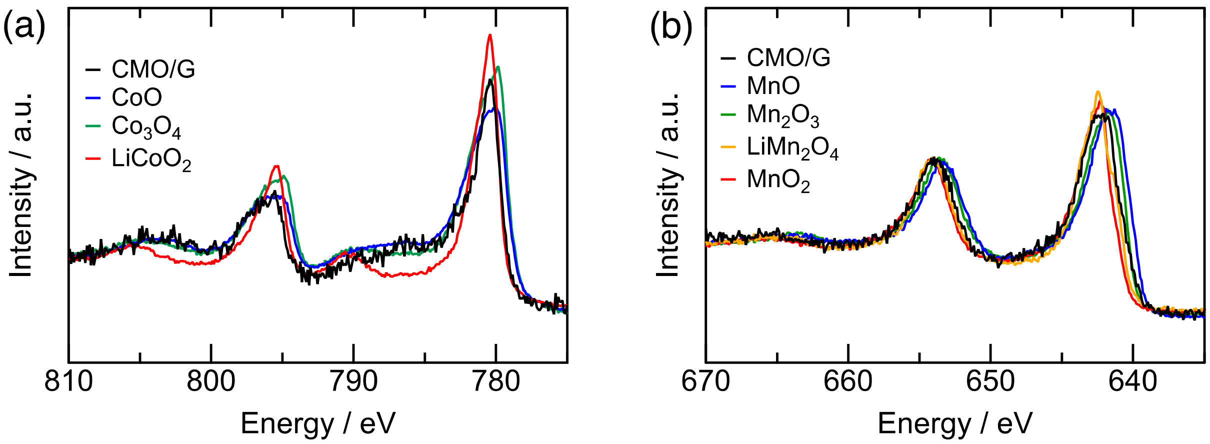

Fig. S3 (a) Co 2p and (b) Mn 2p XPS spectra.

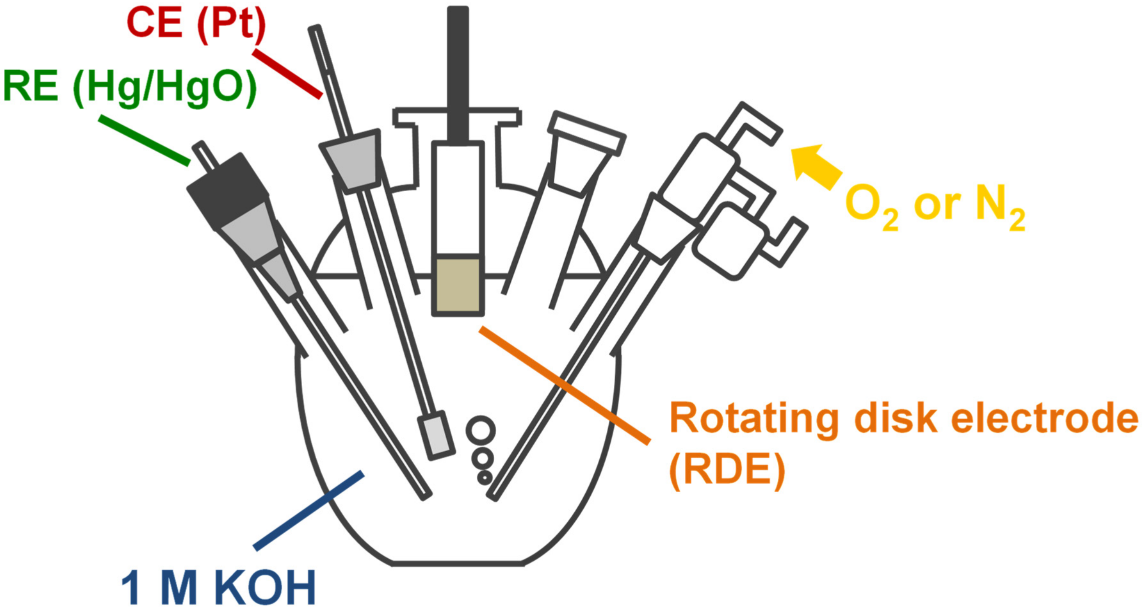

Fig. S4 Setup for the electrochemical measurements in this study.

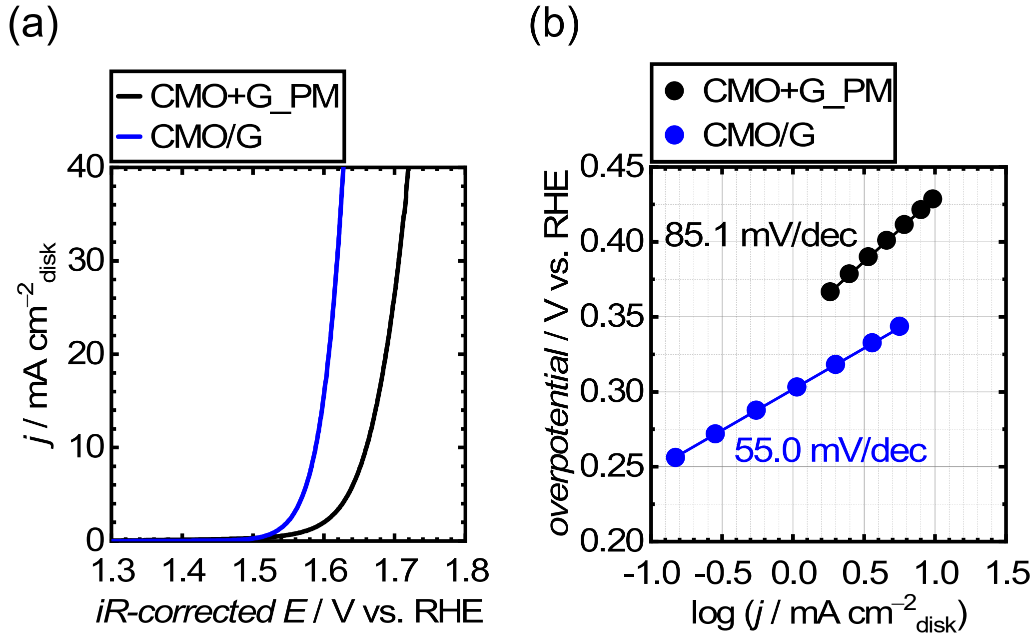

Fig. S5 OER polarization curves per electrode disk area and complementary Tafel plots of CMO/G and CMO + G_PM.

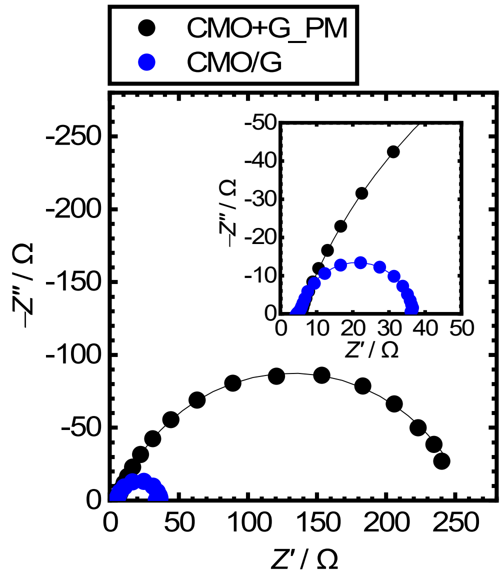

Fig. S6 Nyquist plots from EIS for CMO/G and CMO + G_PM with an inset of magnified spectra collected from 0.1 MHz to 0.1 Hz at 1.60 V vs RHE in O_2-saturated 1 M KOH.

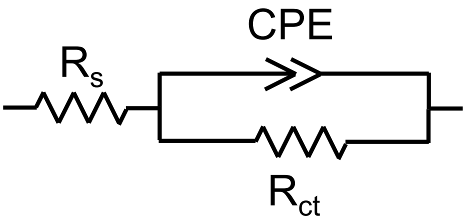

Fig. S7 Equivalent circuit to fit the collected Nyquist plots. Each element represents R_s: solution resistance; R_{ct}: charge-transfer resistance; CPE: constant phase element.

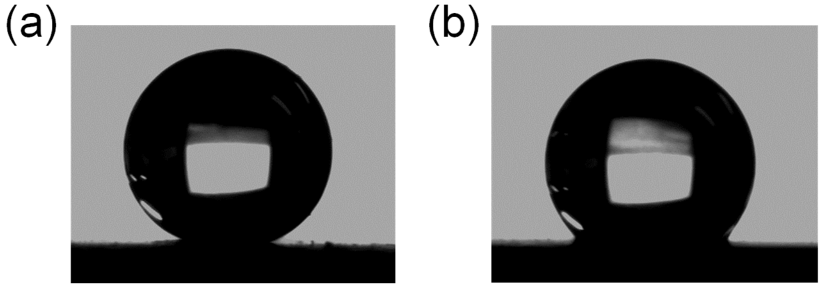

Fig. S8 Water static contact angles on the (a) CMO + G_PM and (b) CMO/G inks, coated on glassy carbon.

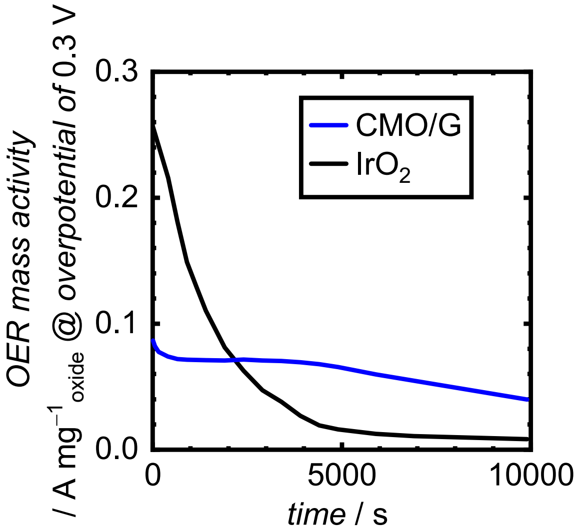

Fig. S9 Change in the OER mass activity at the overpotential of 0.3 V after corresponding time for each potential cycle number for CMO/G and benchmark IrO_2 in N_2-saturated 1 M KOH.

Table S1 Characterization results of CMO/G and CMO.

Material	Diameter[a] [nm]	Metal composition[b] [wt%]	CMO:Graphene[c] [wt%]
CMO	200–300	Co 39.8, Mn 60.2	–
CMO/G	40–80	Co 36.6, Mn 63.4	59:41

[a]Estimated by SEM images. [b]Quantified by ICP-AES analysis. [c]Quantified by CHN analysis.

Table S2 OER mass activities of the previously reported multimetallic oxide-based electrocatalysts containing first-row transition metals.

catalyst	mass activity @1.60 V[a] [A mg^{-1}_{oxide}]	ref
CMO/G	0.26	this work
CMO + G_PM	3.9×10^{-3}	this work
$CoMn_2O_4$/Vulcan carbon	3.7×10^{-3}	3
$MnCo_2O_4$/Vulcan carbon	6.7×10^{-3}	3
$CoFe_2O_4$/rod-like mesoporous carbon	3.4×10^{-2}	4
$NiCo_2O_4$/Vulcan carbon	1.7×10^{-2}	5
$NiMn_2O_4$	2.6×10^{-3}	6
$MnCo_2O_4$/Vulcan carbon	1.8×10^{-2}	7
$MnCo_2O_4$/N-doped carbon nanofiber	2.4×10^{-2}	8
$MnFe_2O_4$/Vulcan carbon	3.3×10^{-3}	9
$CoFe_2O_4$/Vulcan carbon	6.7×10^{-3}	9
$NiFe_2O_4$/Vulcan carbon	6.7×10^{-3}	9
$NiCo_2O_4$	5.0×10^{-2}	10
$Co_{0.2}Ni_{0.2}Fe_{0.6}Fe_2O_4$/carbon black	0.19	11

[a] Calculated by measured currents at 1.60 V in OER polarization curves and loading amount of oxide on the RDE.

Table S3 OER mass activities of the previously reported multimetallic oxide-based electrocatalysts containing first-row transition metals coupled with graphene derivatives.

catalyst	mass activity @1.60 V[a] [A mg^{-1}_{oxide}]	ref
CMO/G	0.26	this work
$MnCo_2O_4$/N-doped reduced graphene oxide	1.0×10^{-2}	12
$CoFe_2O_4$/reduced graphene oxide	5.3×10^{-3}	13
$FeCo_2O_4$/hollow graphene sphere	6.0×10^{-3}	14
$CoFe_2O_4$/reduced graphene oxide	8.7×10^{-3}	15
$(Ni_2MnCo_2)xOy$/reduced graphene oxide	0.11	16
$NiCoMnO_4$/N-doped reduced graphene oxide	1.6×10^{-2}	17
$FeCoNiO_x$/N-doped graphene	0.11	18

[a] Calculated by measured currents at 1.60 V in OER polarization curves and loading amount of oxide on the RDE.

Supporting Reference

1 Y. Sugawara, H. Kobayashi, I. Honma and T. Yamaguchi, *ACS Omega*, 2020, **5**, 29388–29397.

2 Y. G. Li, W. Zhou, H. L. Wang, L. M. Xie, Y. Y. Liang, F. Wei, J. C. Idrobo, S. J. Pennycook and H. J. Dai, *Nat. Nanotechnol.*, 2012, **7**, 394–400.

3 P. W. Menezes, A. Indra, N. R. Sahraie, A. Bergmann, P. Strasser and M. Driess, *ChemSusChem*, 2015, **8**, 164–171.

4 P. X. Li, R. G. Ma, Y. Zhou, Y. F. Chen, Z. Z. Zhou, G. H. Liu, Q. Liu, G. H. Peng, Z. H. Liang and J. Wang, *J. Mater. Chem. A*, 2015, **3**, 15598–15606.

5 J. Wang, Z. X. Wu, L. L. Han, R. Q. Lin, H. L. L. Xin and D. L. Wang, *ChemCatChem*, 2016, **8**, 736–742.

6 X. B. He, F. X. Yin, Y. H. Li, H. Wang, J. N. Chen, Y. H. Wang and B. H. Chen, *ACS Appl. Mater. Interfaces*, 2016, **8**, 26740–26757.

7 W. H. Wang, L. Kuai, W. Cao, M. Huttula, S. Ollikkala, T. Ahopelto, A. P. Honkanen, S. Huotari, M. K. Yu and B. Y. Geng, *Angew. Chem. Int. Ed.*, 2017, **56**, 14977–14981.

8 D. Bin, Z. Y. Guo, A. G. Tamirat, Y. Y. Ma, Y. G. Wang and Y. Y. Xia, *Nanoscale*, 2017, **9**, 11148–11157.

9 C. H. Si, Y. L. Zhang, C. Q. Zhang, H. Gao, W. S. Ma, L. F. Lv and Z. H. Zhang, *Electrochim. Acta*, 2017, **245**, 829–838.

10 J. Bejar, L. Alvarez-Contreras, J. Ledesma-Garcia, N. Arjona and L. G. Arriaga, *J. Electroanal.*

Chem., 2019, **847**, 113190.

11 V. N. Archana, P. K. Rastogi, S. Thoufeeq, S. Vinayasree, S. Shaji, V. R. Reddy, M. A. Garza-Navarro, S. Thomas, T. N. Narayanan and M. R. Anantharaman, *Sustainable Energy Fuels*, 2020, **4**, 3915–3925.

12 X. M. Ge, Y. Y. Liu, F. W. T. Goh, T. S. A. Hor, Y. Zong, P. Xiao, Z. Zhang, S. H. Lim, B. Li, X. Wang and Z. L. Liu, *ACS Appl. Mater. Interfaces*, 2014, **6**, 12684–12691.

13 W. Y. Bian, Z. R. Yang, P. Strasser and R. Z. Yang, *J. Power Sources*, 2014, **250**, 196–203.

14 Z. Weng, W. Liu, L. C. Yin, R. P. Fang, M. Lo, E. I. Altman, Q. Fan, F. Li, H. M. Cheng and H. L. Wang, *Nano Lett.*, 2015, **15**, 7704–7710.

15 W. N. Yan, X. C. Cao, K. Ke, J. H. Tian, C. Jin and R. Z. Yang, *RSC Adv.*, 2016, **6**, 307–313.

16 R. Miao, J. K. He, S. Sahoo, Z. Luo, W. Zhong, S. Y. Chen, C. Guild, T. Jafari, B. Dutta, S. A. Cetegen, M. C. Wang, S. P. Alpay and S. L. Suib, *ACS Catal.*, 2017, **7**, 819–832.

17 A. Pendashteh, J. Palma, M. Anderson and R. Marcilla, *Appl. Catal. B-Environ.*, 2017, **201**, 241–252.

18 R. Z. Jiang, D. R. Baker, D. T. Tran, J. T. Li, A. C. Leff and S. S. Zhang, *ACS Appl. Nano Mater.*, 2020, **3**, 7119–7129.